



2 **Recent contributions to the optimal design of pipeline**
3 **networks in the energy industry using mathematical**
4 **programming**

5 **Diego C. Cafaro^{1,2}  · Demian J. Presser^{1,2} · Ignacio Grossmann³**

6 Received: 30 December 2021 / Accepted: 25 May 2022
7 © The Author(s) under exclusive licence to Sociedad de Estadística e Investigación Operativa 2022

8 **Abstract**

9 The optimal design of pipeline networks has inspired process systems engineers and
10 operations research practitioners since the earliest times of mathematical program-**AQ1**
11 ming. The nonlinear equations governing pressure drops, energy consumption and
12 capital investments have motivated nonlinear programming (NLP) approaches and
13 solution techniques, as well as mixed-integer nonlinear programming (MINLP) for-
14 mulations and decomposition strategies. In this overview paper, we present a sys-
15 tematic description of the mathematical models proposed in recent years for the
16 optimal design of pipeline networks in the energy industry. We provide a general
17 framework to address these problems based on both the topology of the network to
18 build, and the physical properties of the fluids to transport. We illustrate the compu-
19 tational challenges through several examples from industry collaboration projects,
20 published in recent papers from our research group.

21 **Keywords** Pipeline · Network · Energy · Supply chain · Design · Optimization ·
22 MINLP

23 **List of Symbols**

24 **Sets**

25 A_i Subset of nodes adjacent to node i
26 C Components in the fluid stream
27 D Alternative pipeline diameters

A1  Diego C. Cafaro
A2 dcafar@fiq.unl.edu.ar

A3 ¹ INTEC(UNL-CONICET), Güemes 3450, 3000 Santa Fe, Argentina

A4 ² Fac. de Ing. Química, Universidad Nacional del Litoral, Santiago del Estero 2829,
A5 3000 Santa Fe, Argentina

A6 ³ Department of Chemical Engineering, Carnegie Mellon University, 5000 Forbes Ave.,
A7 Pittsburgh, PA 15213, USA

28	I, J, K, L	Nodes in the network
29	S	Fluid states
30	T	Time periods
31	Parameters	
32	ec_t	Unit energy cost during period t
33	g	Gravity constant
34	glr	Gas-to-liquid ratio in multiphase flows
35	$k_{i,j}$	Constant of the Hazen-William correlation for a pipeline connecting i and j
36		
37	$l_{i,j}$	Length of the pipeline connecting i and j
38	lt	Lead-time for pipeline construction
39	r	Discount rate for cashflows
40	sg, sl	Specific gravity of the gas/liquid
41	s_L	Head loss per unit length for water pipeline design purposes
42	P_o, T_o	Pressure and temperature at standard conditions
43	$tc_{i,j,d}$	Transportation capacity of a pipeline with diameter d connecting i and j
44		
45	$vmax_{LP/GP}$	Maximum linear velocities admitted for liquid and gas phases
46	z	Gas compressibility factor
47	α, β	Parameters of economy-of-scale functions
48	γ	Constant of the Weymouth correlation for gas flows
49	$\delta_{i,j,d}$	Numerical value of the diameter d for a pipeline connecting i and j
50		
51	$\Delta sp_{i,j}^{Max}$	Maximum difference of square pressures allowed between nodes i and j
52		
53	Δt	Length of a time period
54	$\Delta z_{i,j}$	Elevation difference between nodes i and j
55	ε	Roughness of the internal wall of the pipeline
56	ζ	SPE constant for multiphase pipeline sizing
57	η	Pump yield
58	θ	Temperature of the fluid
59	ν	Kinematic viscosity of the fluid
60	μ_c	Relative contribution of component c to the calculation of the pressure drop
61		
62	ρ, ρ_{avg}	Density/average density of the multiphase flow
63	$\varphi_{c,j}$	Fraction of component c removed from the flow stream at node j
64		
65	$\psi_{s,s',i}$	Yield of s' per unit of s processed in node i
66	ω	Exponent of the Hazen-Williams correlation
67	Non-negative variables	
68	$Capex(d_{i,J,t})$	Capital expenditures on a pipeline with diameter d connecting i and j built in period t
69		
70	$d_{i,J,t}$	Diameter of a pipeline connecting i and j built in period t

Recent contributions to the optimal design of pipeline networks...

71	$dl_{i,j,t}$	= $d_{i,j,t}^2$ for liquid pipelines
72	$dg_{i,j,t}$	= $d_{i,j,t}^{2.667}$ for gas pipelines
73	$D_{c,K,t}$	Demand of component c at node k during period t
74	$D_{s,I,t}$	Demand of fluid in state s at node i during period t
75	$C_{s,I,t}$	Amount of fluid in state s processed at node i during period t
76	f	Friction factor
77	$F_{c,I,j,t}$	Amount of component c flowing from i to j during period t
78	$F_{s,I,i',t}$	Amount of fluid in state s flowing from i to i' during period t
79	h_L	Head loss due to friction
80	$I_{s,I,t}$	Inventory level of s at node i at the end of period t
81	NPC	Total net present cost
82	$\text{Opex}(F_{c,I,j,t})$	Operating expenditures of a pipeline carrying F units of c from i to j during period t
83		
84	$P_{i,T}$	Pressure at node i during period t
85	$P_{j,T}^{\text{sq}}$	$P_{i,t}^2$ for gas and multiphase pipelines
86	PW_L	Pump power required to compensate head loss due to friction
87	$Q_{c,I,t}$	Production of component c at node i during period t
88	$Q_{s,I,t}$	Production of fluid in state s at node i during period t
89	$R_{s,I,t}$	Amount of fluid converted into state s at node i during period t
90	Re	Reynolds number
91	$\text{TC}(d, P_{i,t}, P_{j,t})_{i,j,\tau}$	Transportation capacity of a pipeline with diameter d connecting i and j built in period τ , according to inlet and outlet pressures in period t
92		
93		
94	$\text{TC}_{i,j,t}^{\text{oil/gas/water}}$	Transportation capacity of oil/gas/water through pipeline $i-j$ built in period t
95		
96	U	Mean linear velocity of the flow
97	$X_{c,J,t}$	Concentration of c in the flows leaving node j during period t
98	X_{LM}	Lockhart-Martinelli parameter for multiphase flows
99	$\Delta P_{i,j,t}^{\text{sq}}$	Difference of square pressures at nodes i and j during period t
100	$\Delta P_g, \Delta P_l$	Pressure drops for gas and liquid phases in multiphase flows
101	Binary variables	
102	$u_{i,j,t}$	= 1 if the flow direction is from i to j during period t
103	$x_{i,j,d,t}$	= 1 if a pipeline with diameter d is built between i and j in period t
104		

105 1 Introduction

106 The energy industry is currently facing difficult challenges due to increasing com-
 107 petitiveness and narrow profit margins. Besides that, and perhaps more importantly,
 108 the need to adopt cleaner sources that reduce the impact of carbon emissions and

109 freshwater consumption are also unavoidable. In this context, one of the relevant
110 problems that have received increasing attention is the optimal design and manage-
111 ment of pipeline networks. Pipeline network design aims to optimally determine the
112 connections (or links) between a set of nodes, the location of junction points and
113 the diameters of the pipelines (Bhaskaran and Salzborn 1979), while network man-
114 agement is geared towards the operational planning of pipes and facilities to meet
115 demands under customer specifications and contractual rules (Selot et al. 2008).

116 Pipelines have been widely used in the fossil energy industry since 1862. Mod-
117 ern oil and gas (O&G) supply chains comprise extensive networks of pipelines that
118 may carry oil, oil refined products, natural gas, natural gas liquids (NGL), liquefied
119 natural gas (LNG) and methanol, among other energy carriers. In addition, the O&G
120 industry has recently addressed the design of pipeline networks carrying other fluids
121 in large scales for the production of energy. There are two particular problems of
122 current importance in the O&G sector: the supply of freshwater plus the gathering,
123 processing and recycle of produced water to/from unconventional wells for hydraulic
124 stimulation (Cafaro and Grossmann 2020); and the capture, storage, distribution and
125 use of carbon dioxide, mainly to enhance oil recovery from mature fields (Presser
126 et al. 2022). Moreover, the energy industry is looking for cleaner energy carriers that
127 yield lower impacts to the environment but still have a high energy density. That is
128 the case of hydrogen (in liquid or gas state), and related chemicals like ammonia (an
129 easy-handling option in the hydrogen supply chain).

130 Given the benefits of pipelines as transportation means from economic, environ-
131 mental and reliability standpoints (Cafaro and Cerdá 2012), designing efficient net-
132 works of pipelines to aid the sustainable production and supply of energy products
133 is a relevant problem. The main reason why pipeline design decisions are so critical
134 is that they usually imply very large investment costs (in the order of millions of
135 dollars per kilometer of length), and there are substantial benefits from the econo-
136 mies of scale. Thus, sizing pipelines and managing operations in a way that these
137 networks are efficiently utilized is the key to the economic success of many energy
138 projects.

139 According to Mah and Shacham (1978), a pipeline network is a collection of ele-
140 ments such as pipes, compressors, pumps, valves, regulators, heaters, tanks, and res-
141 ervoirs interconnected in a specific way. In their early review on the optimal design
142 of pipeline networks, they distinguish among two parts of the problem that govern
143 the network performance. They can be synthesized as topological and fluid dynam-
144 ics considerations. The first characteristic refers to the way to connect the elements,
145 while the second is determined by physical laws. From the mathematical program-
146 ming perspective, the optimal topology of a pipeline network can be addressed by
147 means of integer programming models, in which the main decisions are represented
148 by 0–1 variables accounting for the installation of a pipeline segment between a pair
149 of the nodes. Pipeline interconnections are usually selected from a superstructure
150 of alternatives (Montagna et al. 2021). Material flows (continuous variables) and
151 balances (linear constraints) are also included in this part of the problem, leading
152 to mixed-integer linear programming (MILP) formulations. These can be viewed
153 as particular cases of the network flow problem, closely related to electrical circuit
154 design and analysis.

155 Besides the combinatorial complexity of the topological problem, the need to
156 simultaneously size the pipelines with the selection of the optimal diameter for every
157 connection makes it even more difficult. Fluid dynamics laws are highly nonlinear,
158 both for liquid and gas streams, yielding complex relations between mass flowrates
159 and pressure losses, according to the pipeline length and diameter. As a result, and
160 generally speaking, the optimal design and operation of pipeline networks leads to
161 mixed-integer nonlinear programming (MINLP) formulations that are computation-
162 ally challenging to solve. That is why as suggested by Mah and Shacham in (1978),
163 not all the questions raised in the pipeline network design and synthesis can be com-
164 pletely and satisfactorily answered. However, great progress has been made in the
165 last decade as it is shown in this contribution.

166 The aim of this paper is to summarize recent contributions and provide a gen-
167 eralized, systematic framework to address pipeline network design problems for the
168 energy industry using mathematical programming. Most of the models described
169 in this work are the results of recent collaboration projects jointly developed at the
170 Center for Advanced Process Decision-Making (CAPD) of the Carnegie Mellon Uni-
171 versity (Pittsburgh, PA, USA) and the INTEC (University of Litoral and CONICET,
172 Santa Fe, Argentina). The projects have been particularly focused in the optimal
173 design and operation of pipeline networks, in close association with industry partners.

174 2 General formulations for pipeline network design

175 Designing a network of pipelines to transport gas and liquids in the energy industry
176 generally comprises three main decisions: (a) how to connect the nodes (pipeline
177 layout), (b) what is the pipeline diameter required for each segment, and (c) what are
178 the flows moving along each pipeline segment during the time horizon. Moreover, as
179 highlighted by Saldanha-da-Gama (2018), the location of structures in a real-world
180 network may require including time as an extra dimension in the decision making
181 process. Indeed, for planning purposes, the time domain is typically discretized in
182 days, weeks, months or quarters. The geographical location of producing sources,
183 potential intermediate nodes and demand sites are usually given, from which the
184 length of each possible connection is known beforehand. However, building a pipe-
185 line to connect each pair of nodes is a decision to be determined. Depending on the
186 number of segments along which the fluids move to reach the destination nodes, one
187 may distinguish between two different types of formulations to optimize the pipe-
188 line network design: (1) mathematical models with a fixed number of steps or “ech-
189 elons”, and (2) formulations with an undetermined number of echelons.

190 2.1 Formulations with a fixed number of echelons

191 These formulations assume that there is a set of nodes i (producers) that need to be
192 connected to one or several second level nodes j (junctions), which in turn need to
193 be connected to one or many third level nodes (e.g., processing nodes), until reach-
194 ing the demand nodes. A simple example for gathering and processing shale gas

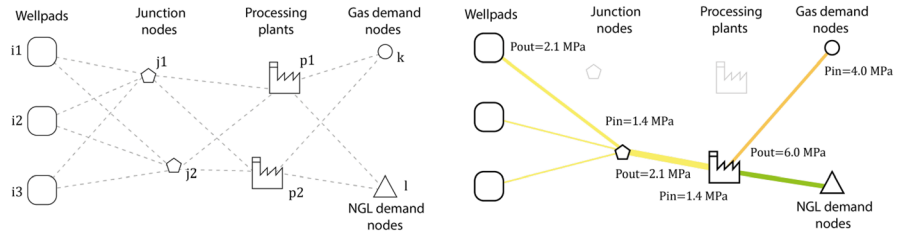


Fig. 1 Simplified superstructure of alternatives (left) and a possible network design in the shale gas supply chain (right), assuming a predefined number of echelons. Pressures are given in 10^6 Pascal (MPa)

195 is presented in Fig. 1. While the left side of Fig. 1 shows all possible connections
 196 between the nodes in the network, the right side shows a feasible solution for this
 197 illustrative problem. It is interesting to note that the product state evolves with each
 198 stage. In the example of Fig. 1, the raw gas produced in nodes i is dehydrated and
 199 compressed in junction nodes j , separated in processing nodes p , and the compo-
 200 nents (natural gas, ethane and LPG) are finally consumed at demand nodes k and l .

201 There are basically two blocks of equations in this formulation, namely mass
 202 balances and pipeline sizing constraints. Mass balances are imposed at every inter-
 203 mediate node (generically denoted by j) and they state that the summation of all
 204 inlet flows (coming from nodes of type i) equals the overall outlet flows (con-
 205 necting to nodes k). That is represented by Eq. (1), in which we assume, for simplicity,
 206 that storing material in the intermediate nodes is not an option. In the most general
 207 case, the streams comprise an overall flow (e.g., natural gas) that is a mixture of
 208 individual components (e.g., methane, ethane, propane, etc.). The set C accounts for
 209 every single component, also including the element $c_o \in C$ that represents the overall
 210 stream. The parameter $\varphi_{c,j}$ is usually used when the node j is a processing facility
 211 where components in the flow are separated from the mainstream. For instance, in
 212 a gas dehydrating unit located at j , $\varphi_{c_o,j} < 1$ since a component in the overall flow
 213 (water) is removed from the stream.

214

$$\varphi_{c,j} \sum_i F_{c,i,j,t} = \sum_k F_{c,j,k,t} \quad \forall j \in J, c \in C, t \in T. \quad (1)$$

215
 216 If the node j is a splitting node, i.e., fractions of the incoming flow are directed to
 217 two or more destinations, extra considerations should be made to manage the mix-
 218 ture of components. To ensure a homogeneous distribution of the component flows
 219 that mix at node j , the bilinear Eq. (2) is included in the formulation.

220

$$F_{c_j,k,t} = X_{c_j,t} F_{c_o,j,k,t} \quad \forall j \in J, k \in K, c \in C - \{c_o\}, t \in T. \quad (2)$$

221
 222 Variable $X_{c_j,t}$ is the concentration of c per unit volume of fluid pooled at node j
 223 during time period t . Since the index c_o accounts for the overall stream (i.e., includ-
 224 ing all components), the right-hand side of Eq. (2) yields the flowrate of the individ-
 225 ual component c from j to k during period t . Hellemo and Tomasgard (2015) present
 226 a generalized MINLP formulation for the pooling problem, where flows of different

227 components, subproducts and products are allocated to intermediates points in a
 228 pipeline network before being delivered to terminal points under specific quality
 229 constraints. Note that Eq. (2) leads to a nonconvex optimization problem that makes
 230 it difficult to search for the global optimal solution. This equation is usually avoided
 231 when: (a) the fluid being transported is not a mixture of components, (b) there is no
 232 need to track individual components but simply the overall flow, or (c) all the flows
 233 gathered at j need to converge to a single node k (no splitting assumption).

234 The second block of constraints deals with the pipeline sizing and installation.
 235 In general terms, if the model selects the link $i-j$ at period t , that pipeline segment
 236 must be available by that time. Moreover, the magnitude of the flow should be
 237 less or equal to the pipeline transportation capacity between nodes i and j , as
 238 imposed by constraint (3). Note that this transportation capacity is a function of
 239 the pipeline diameter d , the fluid state and the pressures at the inlet and outlet
 240 extremes of the segment $(P_{i,t}, P_{j,t})$. The way to calculate the transportation capac-
 241 ity of a pipeline installed in period τ , namely $TC(d, P_{i,t}, P_{j,t})_{s,i,i',\tau}$, is addressed in
 242 detail in upcoming sections.

$$243 \quad \sum_c \mu_c F_{c,i,j,t} \leq \sum_{\tau \leq t-lt} TC(d, P_{i,t}, P_{j,t})_{i,j,\tau} \quad \forall i \in I, j \in J, c \in C, t \in T. \quad (3)$$

244
 245 The value of the parameter μ_c is a modeler's choice, based on the procedure
 246 followed to calculate the transportation capacity. For instance, in most natural gas
 247 gathering networks, $\mu_{c_o} = 1$ and $\mu_c = 0$ for all $c \neq c_o$, meaning that the transporta-
 248 tion capacity simply restricts the overall flow. Instead, in oil gathering networks,
 249 $\mu_{oil} = 1$ while $\mu_{gas} = \mu_{water} = 0$, meaning that the transportation capacity is given
 250 in terms of the oil flowrate (Montagna et al. 2021), even though the flow is also
 251 comprised by water and gas phases. We note that the latter assumption relies on
 252 the condition of constant flow compositions. In Eq. (3) It is the lead time to build
 253 the pipeline segment, given as an integer number of time periods.

254 Finally, production and demand constraints are imposed at the sources i and
 255 destination nodes k , respectively, as expressed through Eqs. (4) and (5). Depend-
 256 ing on the problem goal, only one of these constraints is usually binding at the
 257 optimum. Furthermore, in problems in which the network design is integrated to
 258 the development planning, the production rate Q and/or the demand rate D are
 259 decision variables to be optimized. Since this work is focused on the design of
 260 pipeline networks, we refer the reader to the contributions by Cafaro and Gross-
 261 mann (2014a) and Cafaro and Grosssmann (2020) for further details on how to
 262 model the planning of tasks like drilling, stimulation, completion and production,
 263 from which demand and/or production rates are obtained.

$$264 \quad \sum_j F_{c,i,j,t} = Q_{c,i,t} \quad \forall i \in I, c \in C, t \in T, \quad (4)$$

$$266 \quad \sum_j F_{c,j,k,t} = D_{c,k,t} \quad \forall k \in K, c \in C, t \in T. \quad (5)$$

267

268 If the formulation is strictly concerned with the pipeline network design,
 269 the objective function usually comprises capital and operating costs. These are
 270 brought to the present time to obtain the minimum net present cost. A general
 271 form of that function is given by Eq. (6), where r is the discount rate. Pipeline
 272 capital costs (Capex) are usually dependent on the diameter $d_{i,j,t}$ being selected
 273 to connect nodes i and j (built in period t), while operating costs (Opex) can be
 274 calculated from the material flows $F_{c,i,j,t}$ carried at every single period. Note that
 275 Capex and Opex are non-negative variables defined by model decisions.

276

$$\text{Min NPC} = \sum_t (1 + r)^{-t} \left[\sum_{i,j} \text{Capex}(d_{i,j,t}) + \sum_{i,j,c} \text{Opex}(F_{c,i,j,t}) \right]. \quad (6)$$

277
 278 The way to calculate variables Capex and Opex also depends on the nature of
 279 the problem. In Sect. 3, we present alternative formulations for different fluids (liq-
 280 uid, gas, multiphase), under different assumptions (discrete or continuous values for
 281 pipeline diameters, known or unknown pressures at inlet and outlet sections, etc.).
 282 A general MINLP formulation for pipeline network design, given a fixed number
 283 of echelons to connect production with consumption nodes, will seek to minimize
 284 function (6) subject to constraints (1) to (5).

285 2.2 Formulations with an undetermined number of echelons

286 These formulations can be regarded as generalizations of the previous approaches.
 287 In this case we assume that there is a set of nodes i (either sources, intermediate and/
 288 or demand nodes) that need to be connected to one or more nodes i' in the same set,
 289 which in turn need to be connected to nodes i'' , until reaching the final destination
 290 nodes (see Fig. 2). In any of these nodes, facilities for merging, splitting, storing,
 291 separating and/or processing flows should be installed to make the product flows be
 292 ready for delivery or use. One of the major differences with regards to the models
 293 with a fixed number of echelons is that the flow direction may be reversed in any
 294 pipeline segment over the time horizon.

295 Similar to the models with a fixed number of echelons, mass balance equations
 296 are key constraints of these formulations. Equation (7) states that the overall inven-
 297 tory level at a certain node can be tracked over time by adding flows $F_{s,i',i,t}$ coming
 298 from adjacent nodes $i' \in A_i$, removing the streams $F_{s,i,i'',t}$ derived to other locations
 299 i'' , subtracting the amounts $D_{s,i,t}$ and $C_{s,i,t}$ consumed in the same node i , and adding
 300 the amounts $R_{s,i,t}$ and $Q_{s,i,t}$ produced in that node during the same time period t . In
 301 this case, we model the equations considering material storage, but for simplicity,
 302 we omit the index c of individual components. Model extensions to track the flow
 303 composition are straightforward but might require including bilinear constraints,
 304 as explained in the previous section (for more details, see Cafaro and Grossmann
 305 2020).

306

$$I_{s,i,t} = I_{s,i,t-1} + \sum_{i' \in A_i} F_{s,i',i,t} - \sum_{i'' \in A_i} F_{s,i,i'',t} - D_{s,i,t} - C_{s,i,t} + Q_{s,i,t} + R_{s,i,t} \quad \forall s \in S, i \in I, t \in T. \quad (7)$$

307

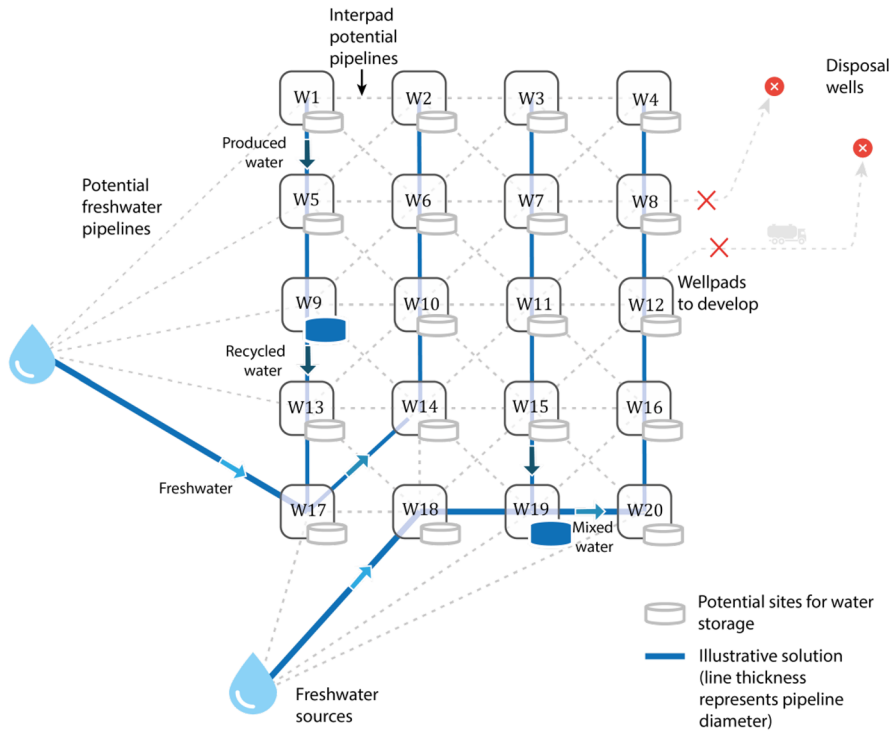


Fig. 2 Superstructure of alternatives for the design of water pipeline networks over a shale gas development area, with no predefined number of echelons

308 Although the indices for individual components are omitted, Eq. (7) includes
 309 the additional index s accounting for product states. If a processing facility is
 310 installed at node i , the consumption of material in state s (e.g., raw gas) may be
 311 associated with the production of s' (e.g., dry gas) in the same node, as denoted
 312 by Eq. (8), where $\psi_{i,s,s'}$ is the yield of s' per unit of s processed in node i . Fig-
 313 ure 3 conceptually illustrates the links between the different product states (layers
 314 in Fig. 3) and their corresponding pipeline networks within the proposed model
 315 structure. Note that layers do not necessarily correspond to different installation
 316 depths of the pipelines below the ground.

317
$$R_{s',i,t} = \sum_s \psi_{s,s',i} C_{s,i,t} \quad \forall s' \in S, i \in I, t \in T. \quad (8)$$

318
 319
 320 Note that in Eq. (7) there are two terms accounting for the production of materi-
 321 al in state s , which are represented by the variables $Q_{s,i,t}$ and $R_{s,i,t}$. In the first
 322 case, the additional material flow comes from external sources (e.g., well produc-
 323 tion); while in the second case, it results from processing other states in the same

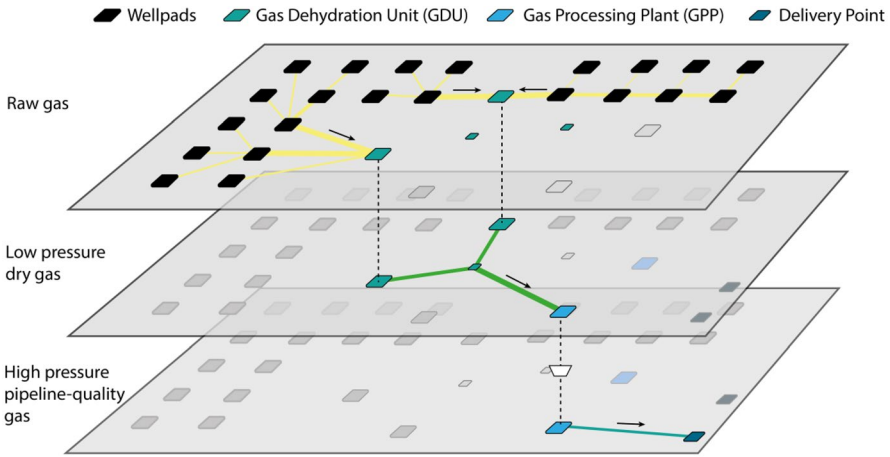


Fig. 3 Conceptual Illustrative example of a natural gas gathering network presenting one layer for each state (raw gas, low pressure dry gas, high pressure pipeline-quality gas) and its corresponding pipeline network

node i . In the most general case, external production $Q_{s,i,t}$ could be also dependent on the development planning.

Similarly, product consumption may be due to external demand $D_{s,i,t}$ or due to processing (change of state), which is represented by $C_{s,i,t}$. In summary, optimization models with no determined number of echelons yield “ s ” different layers of the pipeline network, one for each product state. Links between these networks are the processing facilities at the nodes, where the state of the products may change (for more details, see Montagna et al. 2022).

The second block of constraints accounts for pipeline sizing, imposing an upper bound on the flow of product in state s that is directed from i to i' during period t . More details on how to calculate the transportation capacity $TC(d, P_{i,t}, P_{i',t})_{s,i,i',\tau}$ according to the pipeline diameter, pressures and product state are given in later sections.

$$F_{s,i,i',t} \leq \sum_{\tau \leq t-t} TC(d, P_{i,t}, P_{i',t})_{s,i,i',\tau} \quad \forall i \in I, i' \in A_i, s \in C, t \in T. \quad (9)$$

Although the model, under these constraints, does not strictly avoid bidirectional flows during the same time period (i.e., $F_{s,i,i',t} > 0$ while $F_{s,i',i,t} > 0$), this is discouraged by the operating costs term in the objective function (10) to be minimized. More specifically, one will unnecessarily pay for the transportation of the same material in both directions, yielding the same results in the mass balances. In particular cases, however, binary variables are required to explicitly determine the flow directions. This is also described in further sections.

$$\text{Min NPC} = \sum_t (1+r)^{-t} \left[\sum_{i < i'} \text{Capex}(d_{i,i',t}) + \sum_{i,i',s} \text{Opex}(F_{s,i,i',t}) \right]. \quad (10)$$

348 Finally, the general MINLP formulation for pipeline network design with no pre-
349 defined number of echelons seeks to minimize function (10) subject to constraints
350 (6)–(9).

351 **3 Calculations of the maximum admissible flows, capital** 352 **and operating costs**

353 From the previous formulations, questions that still remain open are the follow-
354 ing: (1) how to estimate the transportation capacity of the pipelines according to
355 diameters and pressures, and (2) how to calculate capital and operating costs. In this
356 section, we describe mathematical models to address these terms, distinguishing
357 between liquid pipelines, gas pipelines, and multiphase (liquid + gas) pipelines.

358 **3.1 Liquid pipeline networks**

359 One of the most widely studied problems involving liquid pipelines is the optimiza-
360 tion of water distribution networks where water demand rates at different nodes are
361 given parameters (Caballero and Ravagnani 2019). However, there are problems for
362 which water is a dependent demand item because its requirement is driven by the
363 operations plan, which is a model decision (e.g., the demand of water at different
364 wells for hydraulic stimulation depends on the development plan). That is why, in
365 the most general case, the demand and/or production of water, oil, NGL (natural gas
366 liquids), LNG (liquefied natural gas), methanol, liquid hydrogen, ammonia, or any
367 other substance in liquid state, may also be model variables (Cafaro and Grossmann
368 2020). Their values depend on the operations plan to be determined by the model,
369 while the pipeline network should be optimally sized together with that plan. Fol-
370 lowing industry practices, the pipeline diameter to select usually belongs to a set of
371 available commercial diameters with specific costs per unit length (Bragalli et al.
372 2012; Araya et al. 2018), but there are works that relax the latter assumption (Cafaro
373 and Grossmann 2014a).

374 Another common assumption in the design of liquid pipeline networks is the sim-
375 plification of hydraulic and pressure calculations. Although they are relevant vari-
376 ables in daily operations, from the standpoint of a process designer they might be
377 simplified. This is based on the incompressibility assumption for liquid flows at rela-
378 tively low pressures, and on the cost of centrifuge pumps, which is generally low in
379 comparison to the pipelines layout.

380 According to Cafaro and Grossmann (2020), liquid pipeline designers usually
381 allow a maximum head loss per unit of length ($s_L = h_L/L$), thus leading to a maxi-
382 mum flow rate for every link i – j that increases with the pipeline diameter ($d_{i,j}$). In
383 the following sections we present the details of this relationship for two particular
384 cases of the energy industry: (1) the design of oil, NGL, and multiproduct pipelines,
385 and (2) water pipeline networks for the development of unconventional resources.

386 3.1.1 Oil and refined product pipeline networks

387 When sizing liquid phase pipelines, petroleum engineers seek to avoid corrosion,
388 erosion and water hammer effects, among other negative phenomena associated with
389 the flow velocity. Based on that, they usually impose a maximum mean velocity
390 ($v_{\max_{LP}}$) of around 1.5 m/s (Society of Petroleum Engineers 2006). Equation (11)
391 determines the maximum flow for oil and other liquids when linking separation
392 facilities (i) with delivery points (j) through a pipeline of diameter $d_{i,j,t}$ installed in
393 time period t . In other words, in the oil industry the maximum admissible flow is
394 usually assumed to be directly proportional to the pipeline cross section.

$$395 \quad TC_{i,j,t}^{\text{oil}} = v_{\max_{LP}} \cdot \frac{\pi}{4} \cdot d_{i,j,t}^2 \quad \forall i \in I, j \in J, t \in T. \quad (11)$$

396
397 In the particular case of ethane and other natural gas liquids (NGL), Cafaro and
398 Grossmann (2014a) propose an equation to convert from volume to mass units. In
399 essence, the fundamentals are the same since the liquid density is assumed to be
400 constant regardless of the pipeline pressure.

401 However, in a more realistic problem representation, pipeline diameters need to
402 be selected from a finite set of alternatives, as proposed by Drouven and Grossmann
403 (2016). Then, Eq. (11) can be modified to impose a different transportation capac-
404 ity according to the diameter of the pipeline installed between i and j in time period
405 t . That is represented by Eq. (12), where $x_{i,j,d,t}$ is a 0–1 variable that equals 1 if and
406 only if a pipeline with diameter δ_d is installed between i and j at period t .

$$407 \quad TC_{i,j,t}^{\text{oil}} = \sum_d tc_{i,j,d} \cdot x_{i,j,d,t} = \sum_d v_{\max_{LP}} \cdot \frac{\pi}{4} \cdot \delta_{i,j,d}^2 \cdot x_{i,j,d,t} \quad \forall i \in I, j \in J, t \in T. \quad (12)$$

409 Assigning binary variables to identify individual alternatives for the pipelines,
410 pumps, compressors and any other element in the network is a way of circumventing
411 the difficulty posed by economies of scale and nonconvex cost functions. The fact
412 that purely nonlinear programming models may not represent the pipeline network
413 design adequately leads to the underlying MINLP model that is usually associated
414 with these problems (Duran and Grossmann 1986). From now on, the equations to
415 be presented assume that the pipeline diameter is a continuous decision variable, but
416 adaptations to the discrete case (as in Eq. 12) are straightforward.

417 Regarding the calculation of capital expenditures, Cafaro and Grossmann (2014a)
418 propose an economy of scale function with the pipeline diameter, which in their
419 model is indeed a continuous decision variable, as presented in Eq. (13). Note that
420 Capex is a non-negative variable determined by the pipeline diameter that is selected
421 by the model.

$$422 \quad \text{Capex}(d_{i,j,t}) = \alpha l_{i,j} d_{i,j,t}^\beta \quad \forall i \in I, j \in J. \quad (13)$$

423
424 In their MINLP formulation, they substitute $d_{i,j,t}^2$ by $dl_{i,j,t}$ in Eq. (11) to keep a lin-
425 ear form in all model constraints, while Eq. (13) is replaced by (13a) and directly
426 introduced in the objective function.

427
$$\text{Capex}(dl_{i,j,t}) = \alpha l_{i,j} d_{i,j,t}^{\beta/2} \quad \forall i \in I, j \in J. \quad (13a)$$

428

429 Note that α and β are given parameters, with $0 < \beta < 1$, leading to a concave cost
 430 function. $l_{i,j}$ is the length of the pipeline segment connecting i and j , which is given,
 431 since the location of the nodes is known beforehand. Pump investment and installa-
 432 tion costs are usually included in this function.

433 Finally, guidelines on how to calculate the operating costs (Opex) in every pipe-
 434 line segment for a given pipeline diameter d can be found in Cafaro et al. (2015).
 435 The authors address the pumping cost for multiproduct liquid pipelines as a func-
 436 tion of the flowrate. Their model assumes that batches move into the pipeline in
 437 plug flow, and interface or "transmix" volumes are neglected. From the relationship
 438 between friction losses and pumping rates by means of Darcy's law (Darcy, 1857)
 439 and Colebrook-White correlation, a nonlinear equation can be used to calculate the
 440 power PW that is required to compensate the friction loss according to the pipeline
 441 diameter and the flowrate at period t . Such a nonlinear equation is then integrated
 442 into the MINLP model (see "Appendix").

443 If the parameter ec_t represents the unit energy cost during the time period t , and
 444 Δt is the period length, pumping charges are given by Eq. (14), which also includes
 445 a linear term accounting for the elevation difference between nodes i and j . Note that
 446 $\Delta z_{i,j} = -\Delta z_{j,i}$, which implies that the cost of pumping fluids in one direction may be
 447 different than in the opposite direction, leading to different operating costs. Also,
 448 note that the latter term (due to gravity) is usually much smaller than the pressure
 449 drop due to friction in large pipeline networks.

450
$$\text{Opex}(F_{i,j,t}) = ec_t [PW_L(F_{i,j,t}, d) + F_{i,j,t} \rho g \Delta z_{i,j}] \Delta t \quad \forall i \in I, j \in J, t \in T. \quad (14)$$

451

452 3.1.2 Water pipeline networks

453 In the particular case of water pipeline networks, the Hazen–Williams correlation
 454 presented in constraint (15) is typically used for design purposes. It assumes that the
 455 maximum admissible flowrate follows a power function with the pipeline diameter.

456
$$TC_{i,j,t}^{\text{water}} = k_{i,j} d_{i,j,t}^{\omega} \quad \forall i \in I, j \in J. \quad (15)$$

457

458 $k_{i,j}$ is a coefficient that depends on the rugosity of the internal walls of the pipeline
 459 and the head loss per unit length of pipe (s_L). Note that, in contrast to oil pipeline
 460 optimization problems, the unit head loss s_L is usually selected a priori, typically
 461 around 10 Pa/m (Caballero and Ravagnani 2019). The exponent ω is empirically
 462 determined by Hazen-Williams at the value of 2.6298.

463 Regarding energy consumption (operating costs), the selection of a fixed s_L for
 464 design purposes yields a simplified, linear formula. This implies that the flowrate is
 465 set at a value such that the head loss per unit length equals s_L . If the pipeline diame-
 466 ter is larger than required ($F_{i,j,t} < TC_{i,j,t}^{\text{water}}$) then the pipeline will be idle for some
 467 time, but the flowrate during active intervals will be fixed at the value mentioned

above. Hence, the pumping costs can be calculated from the friction head loss and elevation difference between the nodes ($\Delta z_{i,j}$), as in Eq. (16).

$$\text{Opex}(F_{i,j,t}) = ec_i \rho g (s_L l_{i,j} + \Delta z_{i,j}) \eta F_{i,j,t} \Delta t \quad \forall i \in I, j \in J, t \in T. \quad (16)$$

It is interesting to note that by fixing the head loss per unit length s_L , the liquid transportation cost is a non-negative variable independent of the pipeline diameter that grows linearly with the flowrate.

3.2 Gas pipeline networks

The first MINLP model to address the optimal design of natural gas pipelines was proposed by Duran and Grossmann (1986). The authors solve an integrated problem in which both the configuration and sizing variables must be selected by the same model. In their seminal approach, the transportation capacity of a segment i - j with diameter $d_{i,j,t}$ is assumed to be given by the Weymouth (1912) correlation, as in Eq. (17).

$$TC_{i,j,t}^{\text{gas}} = \gamma^{-0.5} l_{i,j}^{-0.5} (P_{i,t}^2 - P_{j,t}^2)^{0.5} d_{i,j,t}^{2.667} \quad \forall i \in I, j \in J, t \in T, \quad (17)$$

where

$$\gamma = sg\theta [P_o / (0.375 T_o)]^2. \quad (18)$$

s_g is the gas specific gravity at standard conditions and θ is the average gas temperature. Note that if the input and output pressures (P_i, P_j) are assumed to be known, the gas transportation capacity is a function of the pipeline diameter raised to 2.667. In further sections, we present a generalized model where this assumption is relaxed.

If the pipeline diameter is assumed to be a continuous variable, one may use an economy of scale function like (13) to determine the capital cost of the gas pipeline i - j installed at period t . In that case, by substituting $d_{i,j,t}$ with the variable $dg_{i,j,t} = d_{i,j,t}^{2.667}$, Eq. (17) is converted into a linear constraint, and the capital cost can be approximated by Eq. (19).

$$\text{Capex}(dg_{i,j,t}) = \alpha l_{i,j} dg_{i,j,t}^{\beta/2.667} \quad \forall i \in I, j \in J, t \in T. \quad (19)$$

Drouven and Grossmann (2016) present an adapted form of Eq. (19) to the case in which the pipeline diameters are selected from a finite set of commercial sizes, as shown in Eq. (20).

$$\text{Capex}(x_{i,j,d,t}) = \sum_d l_{i,j} \alpha \delta_d^\beta x_{i,j,d,t} \quad \forall i \in I, j \in J, t \in T. \quad (20)$$

Another interesting note on that work is that a simplified strategy to size gas pipelines is adopted, based on imposing an upper bound to the fluid velocity. The authors suggest that as a rule of thumb, operators strive to ensure that the fluid velocity in

Recent contributions to the optimal design of pipeline networks...

507 gas lines does not exceed 20 m/s to minimize noise emissions and to allow for cor-
 508 rosion inhibition. Thus, a preliminary pipeline sizing is made by relying on that sim-
 509 plified, maximum-velocity specification. However, it is also advisable to use stand-
 510 ard gas flow equations such as the Weymouth or Panhandle correlations to calculate
 511 the pressure drops along individual pipeline segments after preliminary sizing. If
 512 these are beyond tolerable specifications, a larger diameter pipeline may be selected.

513 3.2.1 Fixing pressures at the nodes for design purposes

514 In many contributions addressing the optimal design of gas pipeline networks,
 515 usually based on a fixed number of echelons, reference values for inlet and outlet
 516 pressures at the segments are given beforehand to simplify the pipeline sizing equa-
 517 tions (Cafaro and Grossmann 2014a; Montagna et al. 2021). The values in Fig. 4
 518 are reference pressures proposed by Montagna et al. (2021) for the optimal design
 519 of unconventional oil and gas gathering networks. The underlying assumption is
 520 that the pressure at the wellheads is high enough to make oil, gas and water flow
 521 towards the tank batteries for separation. After the combined flow is separated, the
 522 gas flow is pressurized at the compressors to supply the delivery points in compli-
 523 ance with the requirements. It is important to note that all intermediate pressures are
 524 arbitrarily assumed at some reference level for design purposes (see Fig. 4). How-
 525 ever, the actual pressure drops need to be finally determined after the optimization is
 526 performed, considering the actual flowrates between nodes. Computation of actual
 527 pressures is usually made by detailed flow simulations (Chuen et al. 2017). In the
 528 most general case, only wellpads and compressors (inlet/outlet) pressures are given,
 529 while the others stand for optimization variables that may help to achieve better
 530 solutions, as explained in the following section.

531 3.2.2 Optimizing pressures to improve pipeline utilization

532 In a more general problem, an additional challenge is to track pressures at the nodes
 533 of the gas pipeline network over time. As expressed by Eq. (17), the pipeline transpor-
 534 tation capacity for compressible fluids can be modified by handling pressures. If the
 535 number of segments along which the flow of gas is directed to reach a destination node
 536 depends on the network design (i.e., the number of echelons is not fixed beforehand)
 537 one should accurately define the inlet and outlet pressures at every segment for every
 538 time period. By converting gas pressures into decisions variables to be determined, gas

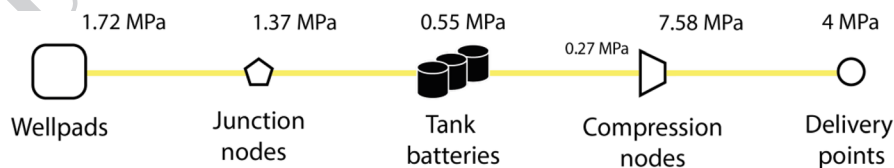


Fig. 4 Reference pressures in 10^6 Pascal (MPa) at different nodes of a network gathering unconventional oil and gas (Montagna et al. 2021)

539 flowrates and flow directions can be optimally handled along the time horizon to make
 540 a better use of the pipeline transportation capacity. Needless to say, though, the math-
 541 ematical formulation becomes more complex.

542 If we raise both sides of the Weymouth correlation presented in Eq. (17), we derive
 543 a quadratic form as in Eq. (21). In this equation, $d_{i,j,t}$ is the diameter of the pipeline con-
 544 necting i to j , already installed at period t .

$$545 \quad \left(TC_{i,j,t}^{\text{gas}} \right)^2 = \gamma^{-1} l_{i,j}^{-1} d_{i,j,t}^{5.334} \left(P_{i,t}^2 - P_{j,t}^2 \right) \quad \forall i \in I, j \in J, t \in T. \quad (21)$$

546 To simplify the formulation, we introduce the variable $P_{i,t}^{\text{sq}} = P_{i,t}^2$ to account for the
 547 square pressure at the node i during period t , which is the actual variable to be opti-
 548 mally set by the model. Note that because pipeline flows can be reversed, it is necessary
 549 to enforce the transportation capacity to be zero when the difference of square pressures
 550 is negative (the gas flows in the opposite direction). This is imposed by Eqs. (22)–(24),
 551 where $u_{i,j,t}$ is a binary variable that takes value one if the gas flows from i to j during
 552 time period t , and zero otherwise.

$$554 \quad u_{i,j,t} + u_{j,i,t} = 1 \quad \forall i \in I, j \in J, t \in T, \quad (22)$$

$$556 \quad \Delta P_{i,j,t}^{\text{sq}} \leq \left(P_{i,t}^{\text{sq}} - P_{j,t}^{\text{sq}} \right) + \Delta sp_{i,j}^{\text{Max}} \left(1 - u_{i,j,t} \right) \quad \forall i \in I, j \in J, t \in T, \quad (23)$$

$$558 \quad \Delta P_{i,j,t}^{\text{sq}} \leq \Delta sp_{i,j}^{\text{Max}} u_{i,j,t} \quad \forall i \in I, j \in J, t \in T. \quad (24)$$

559 $\Delta sp_{i,j}^{\text{Max}}$ is the maximum difference of square pressures for the pipeline segment i – j ,
 560 usually given by the difference between the maximum square pressure at the source i
 561 and the minimum square pressure admitted at the inlet of a junction, compressor or
 562 processing facility.

563 Given that the gas flows, by definition, are greater or equal to 0, the maximum
 564 transportation capacity of a pipeline at a certain time period t can be imposed through
 565 Eq. (25).

$$567 \quad \left(F_{i,j,t} \right)^2 \leq \gamma^{-1} l_{i,j}^{-1} d_{i,j,t}^{5.334} \Delta P_{i,j,t}^{\text{sq}} \quad \forall i \in I, j \in J, t \in T. \quad (25)$$

568 Interestingly enough, if the pipeline diameter is selected from a finite set of alter-
 569 natives, the nonlinear inequality (25) yields a convex quadratic constraint. Then, the
 570 mathematical formulation for the gas pipeline network optimization results in a mixed-
 571 integer quadratically constrained programming (MIQCP) model with a convex relaxa-
 572 tion. Modern solvers like Gurobi 9.0 (Gurobi Optimization LLC 2021) are able to solve
 573 moderate size instances of this problem to global optimality in reasonable CPU times
 574 (Montagna et al. 2022).

576 3.3 Multiphase pipeline networks

577 One of the most difficult challenges in the optimal design of pipeline networks is
 578 when they carry multiphase flows, combining liquid and gas phases. That is the case
 579 of “flowlines” in the oil and gas industry, which gather the wells production (com-
 580 prising oil, gas and water) to separation facilities. Even though there may be more
 581 than two phases in the liquid stream (e.g., oil and water, which are immiscible), they
 582 are usually simplified into a single liquid phase for pipeline sizing purposes (Mon-
 583 tagna et al. 2021). Similarly, for simplicity, in this work we only consider two aggre-
 584 gate phases: liquid and gas.

585 When designing multiphase pipeline networks, the difficulty to calculate pressure
 586 drops comes from the diversity of flow patterns. Figure 5 shows the flow patterns
 587 that are expected according to the velocities of the gas and liquid streams. That is
 588 why pressure drops are usually calculated from empirical correlations. One of the
 589 most widely used procedures is due to Lockhart and Martinelli (1949), while the
 590 Society of Petroleum Engineers (2006) suggests simplified guidelines for multiphase
 591 pipeline sizing that are particularly useful for shorter pipeline segments. Both proce-
 592 dures are detailed in the following section and in the “Appendix”.

593 3.3.1 Multiphase pressure drop prediction and pipeline sizing guidelines

594 The Lockhart–Martinelli procedure (LM) is a widely used method to compute pres-
 595 sure drops on multiphase (liquid and gas) pipelines based on empirical correlations
 596 (Lockhart and Martinelli, 1949). The approach aims to obtain the overall pressure
 597 drop in a straight pipeline segment from the expected pressure drops of the indi-
 598 vidual phases, i.e., as if they were flowing alone. To achieve this, the method com-
 599 putes an intermediate parameter (X_{LM}) as the square root of the ratio between iso-
 600 lated pressure drops, which is subsequently entered on a particular function (Wilkes
 601 2005). This function fits empirical data according to the flow regime of the mul-
 602 tiphase fluid composition, yielding the coefficient Y_G . Finally, the coefficient Y_G is
 603 multiplied by the gas pressure drop to obtain the overall, multiphase pressure drop.

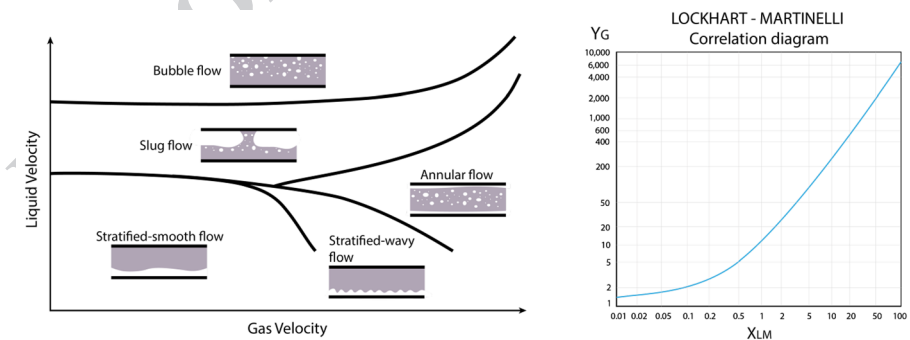


Fig. 5 Two-phase flow patterns and Lockhart–Martinelli correlation diagram to calculate the pressure drops in liquid–gas pipelines

604 Figure 5 shows the correlation diagram that relates the LM parameter (X_{LM}) with the
605 coefficient Y_G under turbulent flow regime. For more details, we refer the reader to
606 the “Appendix”.

607 On the other hand, the Society of Petroleum Engineers (2006) provides guide-
608 lines for the sizing of multiphase pipelines based on admissible flow velocities to
609 prevent erosion, corrosion, noise and water hammer effects. The method imposes an
610 upper bound to the liquid flow rate depending on the pipeline diameter and the gas
611 to liquid ratio, among other physical properties. More details on the SPE guidelines
612 are also given in the “Appendix”.

613 4 Solution strategies

614 The nonlinear equations governing pressure drops, energy consumption and capi-
615 tal investments like the ones presented in this paper have motivated purely nonlin-
616 ear (NLP) approaches and solution techniques, as reviewed by Mah and Shacham
617 (1978). Several years later, the design of gas pipeline networks inspired one of the
618 most valuable contributions to the solution of MINLP problems, namely the outer-
619 approximation algorithm (Duran and Grossmann 1986). The inclusion of binary
620 variables permitted to circumvent the difficulties posed by economies of scale, usu-
621 ally represented by concave cost functions. Such concave cost functions, particularly
622 challenging when sizing pipelines, inspired the development of alternative functions
623 to avoid unbounded gradients in the NLP relaxation (Cafaro and Grossmann 2014b).
624 The latter idea was implemented in the seminal work on the optimal design of shale
625 gas supply chains (Cafaro and Grossmann 2014a), where a Branch-Refine-Optimize
626 (BRO) algorithm allowed to address large-scale instances of the problem.

627 In a more recent contribution, Cafaro and Grossmann (2020) present an itera-
628 tive algorithm searching for better integer solutions in shorter computational times.
629 The procedure implies separating the operations planning from the network design
630 problem to obtain a first approximation to the optimum. If the production planning
631 is prioritized, the required pipeline networks are rather expensive, with oversized
632 capacities. Based on that fact, an interesting way to improve the solution in a second
633 step is to solve the integrated problem but just considering the subset of connections
634 suggested by the original, myopic strategy. Although this subset is relatively large
635 when compared with the optimal design, it excludes many of the connections in the
636 superstructure of alternatives, thus reducing the model size.

637 Following a similar strategy, Montagna et al. (2021) develop a bi-level decom-
638 position procedure that comprises a series of approximations derived from the over-
639 all MINLP model to design pipeline networks with multiphase flows. If solved in
640 a specified sequence, the approximations are able to find efficient solutions to the
641 original problem in modest computational times. The strategy consists in defining
642 NLP formulations comprising all the fluid dynamic equations to estimate the trans-
643 portation capacity of the pipelines, and an MILP formulation for the network design.
644 For any potential multiphase pipeline in the network, an NLP model is solved whose
645 objective is to maximize the admissible flowrate. Such NLP formulations can be
646 regarded as systems of nonlinear equations that can be solved separately, before the

647 network design optimization. Due to their small size, hundreds of these NLP prob-
648 lems can be solved to optimality in few minutes. After that, the MILP approxima-
649 tion relies on the results of the NLP subproblems, taking the resulting transportation
650 capacities as inputs of the pipeline design problem.

651 **5 Illustrative examples**

652 In this section, we illustrate the solutions obtained with the formulations described
653 in this work by means of representative case studies. Case study 1, originally pre-
654 sented by Cafaro and Grossmann (2014a), involves the optimal design of a supply
655 chain network over a shale gas exploitation area, covering more than 10,000 km².
656 Several potential sites for well drilling are considered, assuming different productiv-
657 ity profiles and hydrocarbon composition throughout the region. A network struc-
658 ture with a fixed number of echelons is developed. Case study 2 provides powerful
659 insights on the design of water distribution networks, and confirms the importance
660 of coupling facility sizing decisions with those related to production planning. In
661 contrast to the Case study 1, the network design problem does not impose a fixed
662 number of echelons. A large case study involving 52 wells is described aiming to
663 illustrate the potential of the mathematical formulation. Finally, Case study 3 pre-
664 sents the optimal design of the oil gathering network for unconventional production
665 from a real-world field. The problem statement integrates several decisions such as
666 tank batteries sizing and site selection, pipeline connections and diameters, location
667 of junction nodes and multiperiod investments. A pre-processing NLP formulation
668 is applied to estimate the maximum pipeline transportation capacity for multiphase
669 flows across every possible segment in the superstructure, which is then included in
670 the master MILP model.

671 **5.1 Case study 1: Shale gas pipeline network**

672 The first case study describes the optimal design of a supply chain with a fixed num-
673 ber of echelons in a real world shale play. In their work, Cafaro and Grossmann
674 (2014a) seek not only to define the optimal design of a pipeline network divided
675 in three echelons, but also to determine the optimal drilling and fracturing strat-
676 egy that maximizes the NPV (Net Present Value) of the shale gas project, over a
677 40-quarter planning horizon. A base superstructure comprising a total of 29 nodes
678 with known location is postulated, including 9 potential sites for developing wells,
679 8 potential sites for junction/compression of flows, 3 alternative sites for process-
680 ing plants setup, 3 methane demanding nodes, 3 ethane demanding nodes, and 3
681 freshwater sources (see Fig. 6). All distances between potential nodes, required to
682 compute pipeline lengths and water transportation paths for trucks, are measured in
683 Euclidean norm.

684 The model accounts for several types of pipelines to transport three differ-
685 ent fluids: shale gas, ethane and methane. It also considers the seasonality on
686 natural gas prices and freshwater availability, as well as the economies of scale

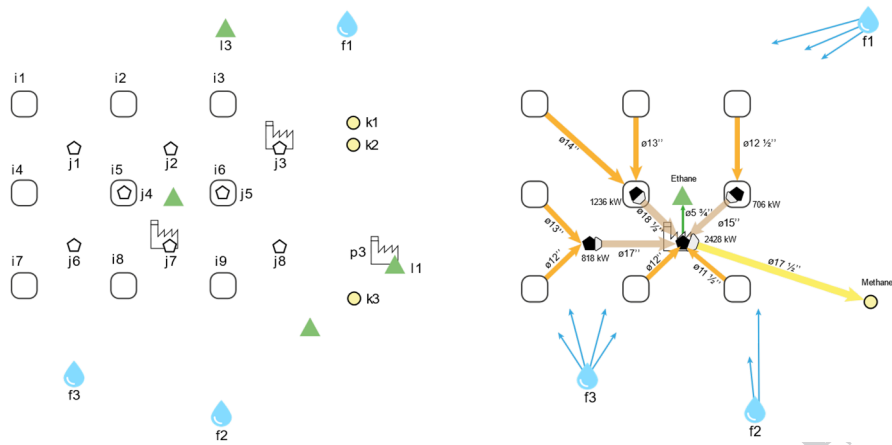


Fig. 6 Base superstructure of nodes and optimal pipeline network design for Case study 1, presented by Cafaro and Grossmann (2014a). Compressors power is given in kilowatts (kW)

687 representing the costs of pipelines, processing plants, wells and compressors. On
 688 the other hand, shale gas productivity at each well is approximated by a discrete-
 689 time decreasing power function of the well age. A variant of the same problem,
 690 including gas “wetness” variability (i.e., different amounts of ethane and NGL in
 691 the gas composition) according to the wellpad location is also addressed.

692 Due to the large size and the computational challenges of the MINLP formula-
 693 tion developed by the authors, a two-level solution strategy is proposed to effi-
 694 ciently tackle the problem. The Branch-Refine-Optimize (BRO) algorithm suc-
 695 cessively refines piecewise-linear underestimations of the concave cost functions.
 696 Since the original MINLP model seeks to maximize the NPV, such MILP relaxa-
 697 tions are solved to find increasingly tighter upper bounds of the objective func-
 698 tion. Feasible solutions are then obtained by solving a reduced MINLP model
 699 that omits network structure variables (potential connections) that take value zero
 700 in the optimal solution of the corresponding MILP approximation. The reduced
 701 MINLP then seeks to improve the lower bounds of the original model. The
 702 MILP-MINLP procedure is repeated until the lower bound (from the MINLP) and
 703 upper bound (from the MILP) are close enough to satisfy an optimization toler-
 704 ance. Using the BRO algorithm, this case study is solved after eight major itera-
 705 tions (using GAMS software and GUROBI 5.5 as the MILP solver, and DICOPT
 706 24.1, combining GUROBI 5.5 and CONOPT 3.15, as the MINLP solver). After
 707 13.7 h of computation on an Intel® Core i7 CPU, 2.93 GHz, 12 GB RAM (with
 708 six parallel threads) the algorithm reports a global optimality gap of 2.5%. The
 709 first MILP model, with piecewise-linear approximations dividing the domain of
 710 concave cost functions into two sectors, is rather large, including 51,888 equa-
 711 tions, 47,643 continuous variables and 3490 binary variables. It takes almost 5 h
 712 of CPU to reach an optimality gap of 0.25% in the same computer. The first MILP
 713 approximation is usually the one that takes the longest time within the BRO algo-
 714 rithm, since there is no integer-feasible solution to start from.

715 The optimal solution yielded by the MINLP formulation of Cafaro and Gross-
716 mann (2014a) is presented at the right of Fig. 6. Results suggest that only one shale
717 gas processing plant is installed in the network. Moreover, optimal shale gas com-
718 pression nodes are established at three junction sites. Finally, the processing plant is
719 linked to a delivery point to supply methane at the required pressure.

720 The optimal solution also suggests that economies of scale are critical, leading
721 to the installation of facilities and pipelines during the first period of the planning
722 horizon, and not expecting any further expansion. Utilization of the processing and
723 transportation facilities peak at time period 7, and remain high for many subsequent
724 periods, as more wells are conveniently developed to steadily deliver the products.
725 Indeed, important conclusions are drawn from this work on how to optimize reser-
726 voir development strategies in coordination with pipeline network designs. By doing
727 so, high utilization levels and stable flows can be obtained over the network.

728 Finally, sensitivity analyses prove that the proposed design is certainly effi-
729 cient, showing significant worsening of the objective function when some changes
730 are enforced in the network configuration (e.g., adding a second processing plant).
731 Furthermore, by extending the model capabilities to consider different gas compo-
732 sitions for different locations over the field, it is demonstrated that the optimal net-
733 work design remains the same, providing important hints on the robustness of the
734 solution.

735 5.2 Case study 2: Water distribution network for shale gas production

736 This example addresses the optimal planning of drilling, fracturing and completion
737 operations together with the optimal design of pipeline networks supplying, process-
738 ing and recycling water for hydraulic fracturing in unconventional gas plays. This
739 is an illustrative case comprising 52 wells to be developed over 12 wellpads, with 2
740 potential sources of freshwater (see Fig. 7). The one-year planning horizon is discre-
741 tized into 52 weekly periods, and there are alternative pipeline diameters and water
742 storage tanks to install in the network. The pipeline connections among the nodes do
743 not need to follow a predefined number of echelons, and flows in pipeline segments
744 (links) may be reversed at different time periods. Due to the combinatorial com-
745 plexity of the overall problem, Cafaro and Grossmann (2020) propose a two-stage
746 decomposition algorithm. The first stage seeks to establish the optimal configuration
747 of the water distribution network having obtained, in advance, the well development
748 plan that maximizes the benefits from gas production. In other words, the water dis-
749 tribution network is subordinated to a so-called “myopic” production plan, from
750 which one determines the water requirements for each of the wellpads over the time
751 horizon. In the second stage, the full optimization model (simultaneously optimizing
752 the production strategy and the network design) is solved, limiting the superstruc-
753 ture of alternatives to the ones suggested by the first stage.

754 The proposed MILP model for Case study 2 comprises 13,567 constraints, 10,586
755 continuous variables and 3251 binary variables. The computational time required
756 for the first stage (myopic solution) is around 145 s, while the simultaneous optimi-
757 zation of well development and water network design and operation, based on the

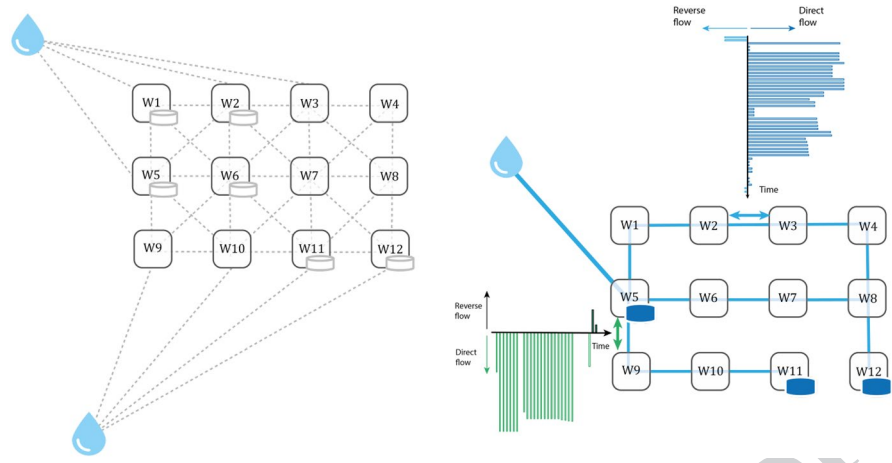


Fig. 7 Superstructure of alternatives for the water distribution network (left) and the optimal network design found by the model proposed by Cafaro and Grossmann (2020) that maximizes the Net Present Value of the project (right)

758 reduced superstructure yielded by the first stage, takes less than 10 min to converge.
759 Instead, the full MILP model with all possible connections takes 27 h to close the
760 optimality gap to 0.4% on an Intel® Core i7 CPU, 12 GB RAM. The best solution
761 found is shown at the right of Fig. 7, and has been obtained using GAMS software
762 with CPLEX 12.9 as the MILP solver, running on 4 parallel threads.

763 Results show that decoupling the operations planning from the pipeline network
764 design may lead to very complex configurations, with numerous pipelines and stor-
765 age facilities to satisfy water demand under myopic, intensive well fracturing plans.
766 In addition, several flow reversals are necessary along the time horizon, leading to
767 higher storage levels and operating costs. In contrast to myopic solutions, simultane-
768 ous optimization yields an improvement of 6% in the NPV (from 101.28 to 107.23
769 million dollars), mainly due to significant savings in water costs at the expense of a
770 less intensive production plan. In fact, a substantial reduction in the water pipeline
771 network complexity is observed, shortening the length of the pipelines by 27%, and
772 reducing water storage capacities by 50%.

773 Finally, the robustness of the pipeline network is tested by admitting more flex-
774 ible field development strategies, where the earliest times to start production in dif-
775 ferent wellpads are shortened. Despite the significant changes in the development
776 plan, the structure of the water distribution network remains unchanged.

777 **5.3 Case study 3: Shale oil gathering network**

778 Montagna et al. (2021) address a real-world case study from the O&G industry
779 involving the optimal design of pipeline networks to gather unconventional oil pro-
780 duction. The authors assume that there is a pre-determined development plan from
781 which operators predict the flows of oil/gas/water to be produced from each well-
782 pad during the following 5 years. The planning horizon is divided into 60 monthly

Recent contributions to the optimal design of pipeline networks...

783 periods and gas-to-oil, and water-to-oil ratios are assumed to remain constant in
 784 time and independent of the wellpad location. In addition, every wellpad is specified
 785 as a potential location for pipeline junction nodes, while potential tank battery loca-
 786 tions are also proposed as possible junction points from where the production can
 787 be transported to the Centralized Delivery Points (CDP). The base superstructure
 788 restricts pipeline connections to a total of four echelons: wellpads–junctions, junc-
 789 tions–tank batteries, tank batteries–junctions, and junctions–CDP (see Fig. 8). The
 790 first two segments carry multiphase flows, while the last two transport single phases,
 791 namely oil, gas and water in separate pipelines.

792 To determine the transportation capacity of multiphase pipelines according to
 793 the length, diameter and flow composition, roughly 2000 NLPs (each involving 21
 794 variables and 15 constraints) are solved using GAMS/IPOPT 30.3 for every segment

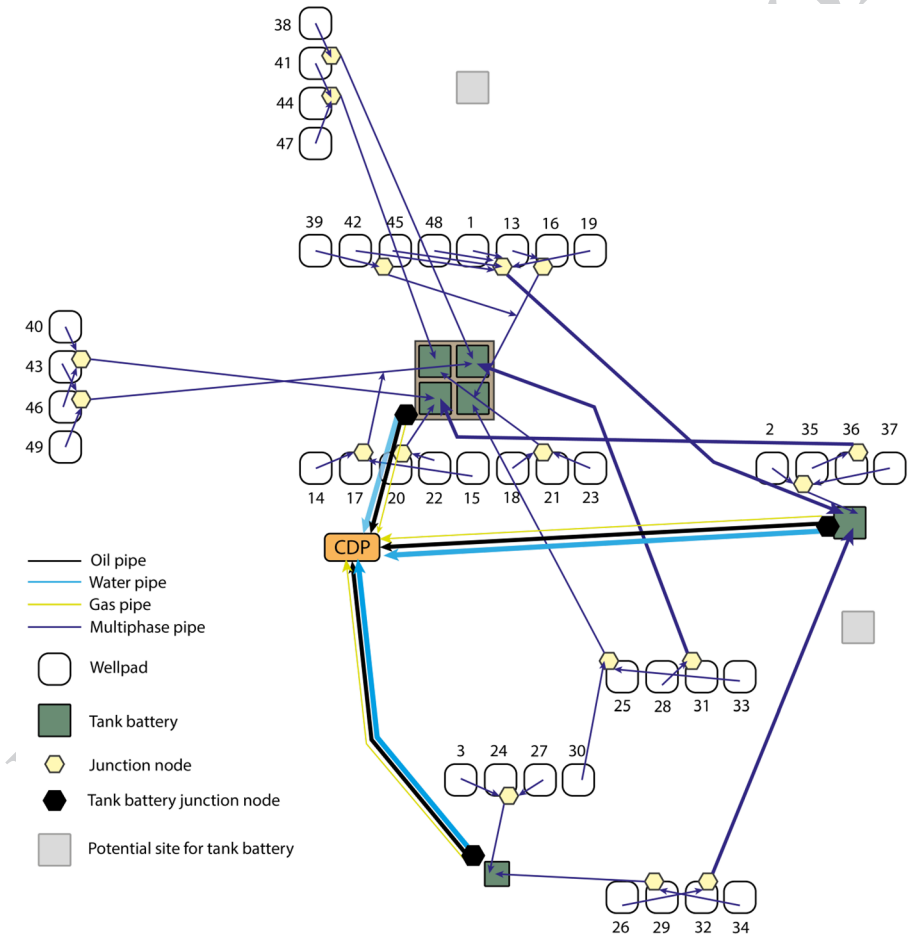


Fig. 8 Gathering network design obtained by Montagna et al. (2021) using a tailored solution algorithm. The number over each wellpad represents the start period of its production, in months

795 in the superstructure. As described in Sect. 4, the NLP models are based on the
796 Lockhart–Martinelli correlation and SPE guidelines, assuming fixed pressures at
797 the intermediate nodes of the network. After solving this pre-processing stage in
798 about 15 min, conservative maximum flowrates are imposed for every triplet ori-
799 gin–destination–diameter, yielding a MILP approximation of the original MINLP
800 that involves 2250 discrete variables, 24,600 continuous variables and 29,441 con-
801 straints after pre-processing. The authors propose an iterative solution algorithm
802 aiming to sequentially provide tighter bounds for the number of tank batteries to be
803 installed and enhance convergence. Making use of the algorithm and after 10 h of
804 computation using the software GAMS/GUROBI 9.0 as the MILP solver, a global
805 optimality gap of 5.2% is achieved, and the best solution found is the one depicted in
806 Fig. 8. All computations have been carried out on an Intel® Core i7 at 3.9 Ghz CPU,
807 with 16 GB RAM, with no parallelization.

808 The gathering network comprises a total of 6 tank batteries, 17 junction nodes
809 spread over the different areas and 3 battery junction points. Different pipeline diam-
810 eters are selected across the network depending on the number of phases in the flow,
811 the transportation distances, and the pressure requirements at the terminal nodes
812 (see thickness of arrows in Fig. 8). Note that despite the apparent complexity of the
813 network design, with many pipeline crossings, such connections are required to keep
814 all the tank batteries with a sufficiently high utilization level, providing substantial
815 savings on facility installation costs. For more details on the timing of investments
816 along the planning horizon and other features of this solution, the reader is referred
817 to the work by Montagna et al. (2021).

818 Although the solution obtained for this case study may still leave room for
819 improvement (the optimality gap is slightly above 5%), it is the first formulation
820 published in the literature that shows the great potential to size pipelines and man-
821 age multiphase flows in the design of pipeline networks. More importantly, it allows
822 obtaining near optimal solutions in reasonable times. The authors conclude that the
823 simultaneous design of the oil gathering network and the definition of production
824 strategies could bring substantial savings to the total investment costs, also stabiliz-
825 ing resource utilization.

826 A summary of the model types and dimensions, solution strategies and computa-
827 tional results for the three case studies is given in Table 1.

828 6 Concluding remarks

829 We have presented a systematic classification of the mathematical models pro-
830 posed in recent years to the optimal design and operation of pipeline networks in
831 the energy industry. To address this problem, the first important question to answer
832 is how to connect the elements of the network, selecting the links from a super-
833 structure of alternatives. We distinguish among two different approaches from the
834 topological perspective: networks with a fixed number of echelons, and networks
835 where the number of echelons is not determined a priori. The second model struc-
836 ture is more flexible, making it possible to reverse the flow direction in some of the
837 segments/links at different time periods to make a better use of the pipelines. In both

Recent contributions to the optimal design of pipeline networks...

Table 1 Problem features, model types, dimensions, solution strategies and computational results for the illustrative case studies

Case Study	Network Design Problem	Fluids	Superstructure size Nodes Echelons	Solution Strategy	Instance	Model Type	Model Size		Solver	CPU time	Global optimality gap	Hardware
							Eqs	Cont. Vars Int Vars				
1	Shale gas supply chain	Shale gas, ethane, methane	29 3	Branch-Refine-Optimize (BRO) Algorithm Iterative: MILP + MINLP	Full problem	MINLP	45,628	44,513	360	BARON 13	24 h	Intel Core i7 CPU 2.93 Ghz, 12 GB RAM, 6 parallel threads
					Piecewise linear approximation	MILP	51,888	47,643	3,490	GUROBI 5.5/ICOPT 24.1 with GUROBI 5.5 and CONOPT 3.15	13.7 h	No Solution 2.50%
2	Water distribution network for shale gas production	Water	14 Undetermined	Decoupling Development Planning and Network Design Iterative: Reduced MILPs	Field Development Strategy, then Network design	MILP	13,567	10,586	1,889	CPLEX 12.9	145 s	Intel Core i7 CPU 2.5 Ghz, 16 GB RAM, 4 parallel threads
					Simultaneous Network design and field development	MILP	13,567	10,586	3,251	CPLEX 12.9	27 h	0.40%

Table 1 (continued)

Case Study	Network Design Problem	Fluids	Superstructure size	Nodes		Echelons	Solution Strategy	Instance	Model Type	Model Size			Solver	CPU time	Global optimality gap	Hardware
				Eqs	Cont. Vars					Int Vars	Eqs	Cont. Vars				
3	Shale oil gathering network work	Multiphase, oil, water natural gas	46	4			Decomposition of MINLP into NLP (maximum admissible flow) and MILP (network design) Two-Stage: NLP + MILP	Full problem	MINLP	59,441	66,600	2,250	BARON 20	24 h	No	Intel Core i7 CPU 3.9 Ghz, 16 GB RAM, no parallel mode
							Maximum admissible flows	NLP		15	21	-	IPOPT 30.3	<1 s	0%	
							Pipeline network design	MILP		29,441	24,600	2,250	GUROBI 9.0	10 h	5.20%	

838 cases, the location of the existing and potential nodes is given and the topology of
839 the network is solved by means of linear integer programming models, in which the
840 main decisions are represented by 0–1 variables accounting for the installation of
841 a pipeline segment between a pair of nodes. The second question is about the size
842 (diameter) of the pipeline to install between the nodes. Sizing pipelines implies the
843 use of fluid dynamics equations to predict the pressure drops, which are strongly
844 nonlinear and dependent on the fluid state. Moreover, economies of scale functions
845 are integrated into these models, yielding mixed-integer nonlinear formulations that
846 are computationally challenging.

847 We have reviewed recent contributions that can be roughly classified accord-
848 ing to the fluid to transport in three groups: liquid pipeline networks, gas pipeline
849 networks, and multiphase pipeline networks. For each of these categories, we have
850 presented alternative models and equations to estimate the pipelines transportation
851 capacity as well as their capital and operating costs. We have described relevant
852 applications of liquid pipeline networks in the energy industry like oil gathering net-
853 works, oil products transmission pipelines and water distribution networks for well
854 stimulation. In turn, we have analyzed recent contributions to the optimal design
855 and operation of natural gas pipeline networks, showing that they can be properly
856 represented by mixed-integer quadratically constrained programming (MIQCP) for-
857 mulations, which is a promising feature given the significant advances of the solu-
858 tion algorithms devised for this particular kind of nonlinear problems in the last few
859 years. Finally, we have highlighted current trends in the optimal design and opera-
860 tion of multiphase pipeline networks, the most complex type of problems that are
861 faced, for instance, when sizing the flowlines that carry a mixture of oil, gas and
862 water from the wellbores to separation facilities over oil and gas fields.

863 The optimal design of pipeline networks has inspired process systems engineers
864 and operations researchers since the early days of mathematical programming. It
865 is not surprising to see that even today it is an active research field that continues
866 inspiring new modeling frameworks and solution strategies. The transportation of
867 liquid and/or gas hydrogen, ammonia, bioethanol, biogas (or renewable natural gas)
868 and any other energy carrier produced from renewable sources represents a new
869 frontier, which will certainly benefit from the developments described in this work.

870 Appendix

871 Calculation of energy consumption in a pipeline segment

872 A method to compute pumping cost for multiproduct pipelines as a function of the
873 flowrate is presented by Cafaro et al. (2015), under the assumption of batch flow
874 and neglecting “transmix” volumes. The mean velocity (U) in a straight segment is
875 given by the ratio between the pump rate and the pipeline section, while the Reyn-
876 olds number is given by $Re = 4F/\pi d\nu$, with ν being the fluid kinematic viscosity. If
877 refined products flow in turbulent regime into the pipeline segments ($Re > 4 \times 10^5$)
878 the relationship between the head loss due to friction (h_f) and the pump rate can
879 be derived from the Darcy’s equation (Darcy 1857) in Eq. (26). This equation

880 introduces the dimensionless friction factor f . Indices of nodes and time periods are
881 omitted for simplicity.

882
$$h_L = f \frac{l U^2}{d 2g} = 8f \frac{l F^2}{d^5 g \pi^2}. \quad (26)$$

883
884 Moreover, the friction factor f can be calculated through the Colebrook-White
885 equation, as in Eq. (27).

886
$$\frac{1}{\sqrt{f}} = -2 \log_{10} \left(\frac{\varepsilon/d}{3.7} + \frac{2.51}{\text{Re} \sqrt{f}} \right). \quad (27)$$

887
888 Equation (27) involves an implicit function accounting for two contributions: the
889 pipeline wall roughness (ε), and the flow turbulence. Finally, the power required to
890 compensate the friction loss is given by Eq. (28), representing a nonlinear function
891 rapidly increasing with the flowrate F .

892
$$\text{PW}_L = \frac{h_L F \rho g}{\eta} = \frac{8\rho}{\pi^2 \eta} \frac{l}{d^5} f F^3. \quad (28)$$

893
894 The parameter ρ is the liquid density, g is the gravitational constant, l is the length
895 of the pipeline and η is the pump efficiency. Equations (29) and (30) are introduced
896 in the MINLP model presented in Sect. 3.1.1 to calculate the energy consumption in
897 every pipeline segment over time period t .

898 **Lockhart–Martinelli procedure to compute pressure drops in multiphase flows**

899 The Lockhart–Martinelli (LM) procedure has been devised to predict the pressure
900 drop for fully developed gas–liquid flows. The first step is to calculate the individual
901 effects of liquid and gas phases, i.e., the pressure drops ΔP_l and ΔP_g that would be
902 expected if the liquid and gas streams were flowing alone through the same pipeline.
903 The second step is to obtain the LM parameter (X_{LM}), as in Eq. (29).

904
$$X_{LM} = \sqrt{\frac{\Delta P_l}{\Delta P_g}}. \quad (29)$$

905
906 Finally, the overall pressure drop in the pipeline segment is estimated from the
907 pressure drop of the gas phase, as in Eq. (30).

908
$$P_{i,t} - P_{j,t} = Y_G \Delta P_g = \left(1 + X_{LM}^{2/n} \right)^n \Delta P_g. \quad (30)$$

909
910 Equation (30) follows the Wilkes function (Wilkes 2005) to fit the data of the
911 LM empirical results. The parameter n depends on the flow regime of each phase,
912 and is equal to 4.12 if both liquid and gas phases flow in turbulent regime, as usu-
913 ally seen in industrial applications. In horizontal pipelines, the pressure drop of
914 the liquid phase ΔP_l can be obtained from the Darcy equation (see Eqs. (31) and
915 (32)), while the gas pressure drop ΔP_g is related to the pipeline diameter and the

916 gas flow through the Weymouth correlation (see Eq. (17) in Sect. 3.2). Note that the
 917 flow rates of the two different phases need to be tracked through separate variables
 918 ($F_{LIQ,i,j,t}$ and $F_{GAS,i,j,t}$), as explained in Sect. 2.1.

919 SPE guidelines for sizing multiphase pipelines

920 Similar to the liquid pipeline sizing problem, the SPE (2006) suggests maximum
 921 velocities for multiphase flows to prevent erosion, corrosion, noise or water ham-
 922 mer effects. Reference maximum velocities are 18 m/s to inhibit noise and 15 m/s
 923 to prevent corrosion. A more accurate procedure to obtain maximum velocities is
 924 suggested as follows.

925 1. Obtain the average multiphase density (ρ_{avg}) from the gas to liquid ratio (glr) as:

$$926 \rho_{avg} = \frac{12409 \text{ sl } P_{in} + 2.7 \text{ glr sg } P_{in}}{198.7 P_{in} + z \text{ glr } \theta}, \quad (31)$$

927 where z is the gas compressibility factor, r the gas/liquid ratio [ft³/bbl], θ the
 928 flow temperature [°R], P_{in} the inlet pressure in PSI, sl the specific gravity of the
 929 liquid phase relative to water, and sg the specific gravity of the gas, relative to
 930 air.
 931 air.

932 2. Set the maximum velocity for the liquid phase as:

$$933 v_{max} = \rho_{avg}^{-0.5}, \quad (32)$$

934 where ζ is an SPE specific constant with a value of 150 for solids-free fluids and
 935 continuous service operation, and v_{max} is measured in ft/s.

937 3. Impose an upper bound on the liquid flowrate, as shown in Eq. (33).

$$938 F_{LIQ,i,j,t} \leq \xi v_{max} d_{i,j,t}^2, \quad (33)$$

$$940 \text{ with } \xi = 0.64516(11.9 + z \text{ glr } \theta / 16.7 P_{in})^{-1}.$$

941 **Acknowledgements** Financial support from National University of Litoral under Grant CAI+D 2020
 942 50620190100163LI, and CONICET under Grant PIP 11220200103053CO is gratefully acknowledged.
 943 Financial support from the Center of Advanced Process Decision-making at Carnegie Mellon University
 944 is also gratefully acknowledged.

945 References

- 946 Araya N, Luca FA, Cisternas LA, Gálvez ED (2018) Design of desalinated water distribution networks:
 947 complex topography, energy production, and parallel pipelines. *Ind Eng Chem Res* 57:9879–9888
 948 Bhaskaran S, Salzborn FJM (1979) Optimal design of gas pipeline networks. *J Oper Res Soc*
 949 30:1047–1060
 950 Bragalli C, D'Ambrosio C, Lee J, Lodi A, Toth P (2012) On the optimal design of water distribution net-
 951 works: a practical MINLP approach. *Opt Eng* 13:219–246
 952 Caballero JA, Ravagnani MASS (2019) Water distribution networks optimization considering unknown
 953 flow directions and pipe diameters. *Comput Chem Eng* 127:41–48

- 954 Cafaro DC, Cerdá J (2012) Rigorous scheduling of mesh-structure refined petroleum pipeline networks.
955 Comput Chem Eng 38:185–203
- 956 Cafaro DC, Grossmann IE (2014a) Strategic planning, design, and development of the shale gas supply
957 chain network. *AIChE J* 60:2122–2142. <https://doi.org/10.1002/aic.14405>
- 958 Cafaro DC, Grossmann IE (2014b) Alternate approximation of concave cost functions for process design
959 and supply chain optimization problems. *Comput Chem Eng* 60:376–380. [https://doi.org/10.1016/j.
960 compchemeng.2013.10.001](https://doi.org/10.1016/j.compchemeng.2013.10.001)
- 961 Cafaro DC, Grossmann IE (2020) Optimal design of water pipeline networks for the development of
962 shale gas resources. *AIChE J*. <https://doi.org/10.1002/aic.17058>
- 963 Cafaro VG, Cafaro DC, Mendez CA, Cerdá J (2015) MINLP model for the detailed scheduling of refined
964 products pipelines with flow rate dependent pumping costs. *Comput Chem Eng* 72:210–221. [https://
965 doi.org/10.1016/j.compchemeng.2014.05.012](https://doi.org/10.1016/j.compchemeng.2014.05.012)
- 966 Chuen CM, Nukman MA, Mandal D, Salim AS, Sepulveda W, Vaca JC, Goh K (2017) Application of
967 allocation algorithm for surveillance and optimization of intelligent wells. In: SPE/IATMI Asia
968 Pacific Oil & Gas Conference and Exhibition. <https://doi.org/10.2118/186421-MS>
- 969 Darcy H (1857) RecherchesExpérimentales Relatives au Mouvement de l'Eau dans les Tuyaux [Exper-
970 mental Research on the Movement of Water in Pipes]. Mallet-Bachelier, Paris
- 971 Drouven M, Grossmann IE (2016) Multi-period planning, design, and strategic models for long-term,
972 quality-sensitive shale gas development. *AIChE J* 62:2296–2323. <https://doi.org/10.1002/aic.15174>
- 973 Duran MA, Grossmann IE (1986) A mixed-integer nonlinear programming algorithm for process systems
974 synthesis. *AIChE J* 32:592–606. <https://doi.org/10.1002/aic.690320408>
- 975 Gurobi Optimization LLC (2021) Gurobi optimizer reference manual
- 976 Hellemo L, Tomasgard A (2015) A generalized global optimization formulation of the pooling problem
977 with processing facilities and composite quality constraints. *TOP* 24:409–444
- 978 Lockhart R, Martinelli RC (1949) Proposed correlation of data for isothermal two-Phase, two-component
979 flow in pipes. *Chem Eng Prog* 45:38–48
- 980 Mah RSH, Shacham M (1978) Pipeline network design and synthesis. *Adv Chem Eng* 10:125–209
- 981 Montagna AF, Cafaro DC, Grossmann IE, Burch D, Shao Y, Wu X-H, Furman K (2021) Pipeline network
982 design for gathering unconventional oil and gas production using mathematical optimization. *Opt*
983 *Eng*. <https://doi.org/10.1007/s11081-021-09695-z>
- 984 Montagna AF, Cafaro DC, Grossmann IE, Ozen O, Shao Y, Zhang T, Guo Y, Wu X-H, Furman K (2022)
985 Surface facility optimization for combined shale oil and gas development strategies. *Comput Chem*
986 *Eng* 2022:2
- 987 Presser DJ, Cafaro VG, Cafaro DC (2022) Optimal sourcing, supply and development of carbon dioxide
988 networks for enhanced oil recovery in CCUS systems. *Comput-Aided Chem Eng* 2022:5
- 989 Saldanha-da-Gama F (2018) Comments on: extensive facility location problems on networks: an updated
990 review. *TOP* 26:229–232
- 991 Selot A, Kuok LK, Robinson M, Mason TL, Barton PI (2008) A short-term operational planning model
992 for natural gas production systems. *AIChE J* 54:495–515
- 993 Society of Petroleum Engineers (2006) Petroleum engineering handbook
- 994 Weymouth TR (1912) Problems in natural gas engineering. *Trans ASME* 34:185–234
- 995 Wilkes JO (2005) Fluid mechanics for chemical engineers. Pearson, Upper Saddle River

996 **Publisher's Note** Springer Nature remains neutral with regard to jurisdictional claims in published maps
997 and institutional affiliations.

998

Journal:	11750
Article:	635

Author Query Form

Please ensure you fill out your response to the queries raised below and return this form along with your corrections

Dear Author

During the process of typesetting your article, the following queries have arisen. Please check your typeset proof carefully against the queries listed below and mark the necessary changes either directly on the proof/online grid or in the 'Author's response' area provided below

Query	Details Required	A u t h o r ' s Response
AQ1	Please provide MSC codes. For more details, if required, kindly visit http://www.ams.org/msc/ .	
AQ2	Kindly provide necessary details for the ref. (Society of Petroleum Engineers 2006; Gurobi Optimization LLC 2021), if possible.	